Supplemental Document

Optics EXPRESS

All-optical wavelength conversion of a 92-Gb/s 16-QAM signal within the C-band in a single thin-film PPLN waveguide: supplement

JUNJIE WEI,[1] ZIHE HU,[2] MINGMING ZHANG,[2] PAN LI,[1] YOU WU,[1] CHENG ZENG,[1,4] MING TANG,[1,2,3,5] AND JINSONG XIA[1,6]

[1] *Wuhan National Laboratory for Optoelectronics, Huazhong University of Science and Technology, Wuhan, 430074, China*
[2] *National Engineering Laboratory for Next Generation Internet Access System, School of Optical and Electronic Information, Huazhong University of Science and Technology, Wuhan, 430074, China*
[3] *Optics Valley Laboratory, Hubei 430074, China*
[4] *zengchengwuli@hust.edu.cn*
[5] *tangming@mail.hust.edu.cn*
[6] *jsxia@hust.edu.cn*

Supplement DOI: https://doi.org/10.6084/m9.figshare.20374803

Parent Article DOI: https://doi.org/10.1364/OE.465382

All-optical wavelength conversion of a 92-Gb/s 16-QAM signal within the C-band in a single thin-film PPLN waveguide: supplemental document

JUNJIE WEI,[1] ZIHE HU,[2] MINGMING ZHANG,[2] PAN LI,[1] YOU WU,[1] CHENG ZENG,[1,4] MING TANG[1,2,3,5] AND JINSONG XIA[1,6]

[1]*Wuhan National Laboratory for Optoelectronics, Huazhong University of Science and Technology, Wuhan, 430074, China*
[2]*National Engineering Laboratory for Next Generation Internet Access System, School of Optical and Electronic Information, Huazhong University of Science and Technology, Wuhan, 430074, China*
[3]*Optics Valley Laboratory, Hubei 430074, China*
[4]*e-mail: zengchengwuli@hust.edu.cn*
[5]*e-mail: tangming@mail.hust.edu.cn*
[6]*e-mail: jsxia@hust.edu.cn*

Details of Cr poling electrodes. The schematic of Cr poling electrodes is shown in Fig. S1(a). And the details of Cr poling electrodes are shown in Table. S1. The electrode duty cycle is the ratio of the electrode teeth width and electrode teeth period. In the center of electrodes is a single periodically poled lithium niobate (PPLN) waveguide, where the dark blue region and light blue region represents the periodic reversed and original ferroelectric domain, respectively. Fig. S1(b) shows the scanning electron microscope (SEM) image of the PPLN waveguide after hydrofluoric acid (HF) wet etching process. In the center of the image is a PPLN waveguide with periodic reversed ferroelectric domain. At a short poling period of 4.41μm, our PPLN waveguides exhibit great periodic poling quality with a duty cycle of

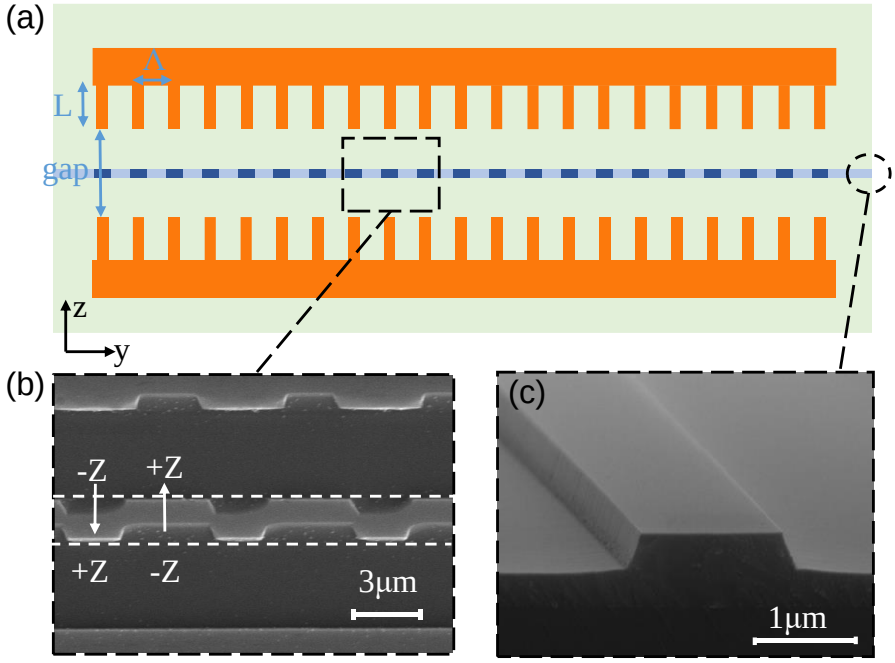

Fig. S1. (a) The schematic of Cr poling electrodes, and a single PPLN waveguide is in the center of electrodes. (b) The scanning electron microscope (SEM) image of the PPLN waveguide after hydrofluoric acid (HF) wet etching process. The original waveguide before HF wet etching is in the white dash region. (c) The SEM image of the waveguide cross section.

Table S1. details of Cr poling electrodes

Electrode geometry	Electrode teeth gap (μm)	Electrode teeth length L (μm)	Electrode teeth period Λ (μm)	Electrode teeth width (μm)	Electrode duty cycle
rectangle	12	6	4.41	1.543	35%

43.9%±2%, which is essential for achieving high conversion efficiencies. Fig. S1(c) shows the SEM image of the waveguide cross section. The waveguide facets are firstly cut by a dicing machine (DS613) and then polished by a chemical-mechanical polishing machine.

All-optical wavelength conversion (AOWC) spectra. In this measurement, the pump (1550.92 nm) and signal waves (1541.35 nm) are coupled into a wavelength division multiplexer (WDM). At the output, idler wave is generated at 1560.68 nm. Figures S2(a) and (b) show the AOWC spectra of cSHG/DFG process with different on-chip pump and signal powers. As the pump power increases, the signal power grows slowly but the idler power grows rapidly, as shown in the inset of Fig. S2(a). The inset of Fig. S2(b) shows that the idler power increases almost the same as the signal power increases.

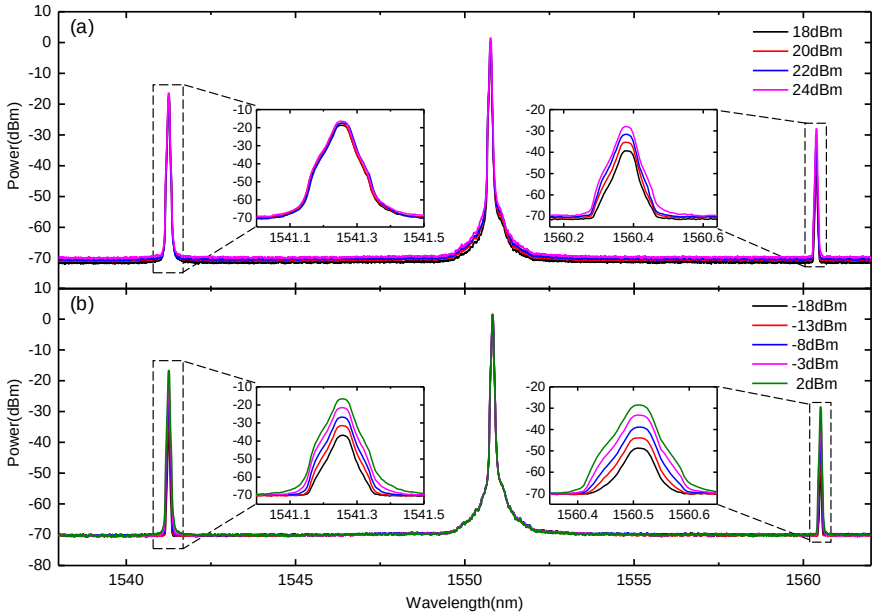

Fig. S2. (a) AOWC spectrum with 18 dBm (black), 20 dBm (red), 22 dBm (blue) and 24 dBm (pink) on-chip pump power, and the on-chip signal power is fixed at 2 dBm. The insets show the detailed signal and idler spectra. (b) AOWC spectrum with -18 dBm (black), -13 dBm (red), -8 dBm (blue), -3 dBm (pink) and 2 dBm (green) on-chip signal power, and the on-chip pump power is fixed at 24 dBm. The insets show the detailed signal and idler spectra.

Energy and momentum conservations for cSHG/DFG process. The cSHG/DFG process involves two distinct nonlinear processes, which are SHG and DFG. For SHG process, a single SH (higher energy) photon is generated by two pump (lower energy) photons due to energy conservation in Eq. (S1). Simultaneously, DFG process is achieved by mixing of an input signal wave with the SH wave. Here, with an input signal photon, the generated SH photon (higher energy) is converted to one idler and one additional signal (two lower energy) photons as shown in Eq. (S2). During the DFG process, the signal wave is amplified and the conjugate idler wave is generated at the different frequency. To achieve high efficiency, quasi-phase matching

(QPM) technique is applied in PPLN waveguides. The phase matching equations and energy conservations of SHG and DFG are given as [1]

$$k_{\mathrm{SH}} - 2k_p - \frac{2\pi}{\Lambda_{\mathrm{SHG}}} = 0, \qquad 2\omega_p = \omega_{\mathrm{SH}}, \tag{S1}$$

$$k_{\mathrm{SH}} - k_s - k_i - \frac{2\pi}{\Lambda_{\mathrm{DFG}}} = 0, \quad \omega_{\mathrm{SH}} + \omega_s = 2\omega_s + \omega_i. \tag{S2}$$

Here, $k_j = n_{\mathrm{eff}}(\omega_j,T)\omega_j/\mathrm{c}$ (j = SH, p, s, i) is the wave-vector at SH (ω_{SH}), pump (ω_p), signal (ω_s) and idler frequency (ω_i), respectively, n_{eff} is the effective refractive index at specific temperature (T) and frequency (ω_j), and c is the speed of light in vacuum. Λ is the poling period of PPLN waveguides. After substituting k_j into Equations (S1) and (S2), the poling periods of SHG and DFG process are

$$\Lambda_{\mathrm{SHG}} = \frac{\lambda_{\mathrm{SH}}}{n_{\mathrm{eff}}(\lambda_{\mathrm{SH}}) - n_{\mathrm{eff}}(\lambda_p)}, \tag{S3}$$

$$\Lambda_{\mathrm{DFG}} = \frac{1}{\dfrac{n_{\mathrm{eff}}(\lambda_{\mathrm{SH}})}{\lambda_{\mathrm{SH}}} - \dfrac{n_{\mathrm{eff}}(\lambda_s)}{\lambda_s} - \dfrac{n_{\mathrm{eff}}(\lambda_i)}{\lambda_i}}. \tag{S4}$$

At room temperature, we obtain the numerically simulated effective refractive indices (n_{eff}) of fundamental transverse-electric (TE_{00}) modes at different wavelengths (λ_j) using the waveguide dimensions. After calculation, we find that $\Lambda_{\mathrm{SHG}} \approx \Lambda_{\mathrm{DFG}} \approx 4.41\mu\mathrm{m}$ within the bandwidth of interest, so that the SHG and DFG processes can simultaneously and efficiently accomplish in a single PPLN waveguide.

Coupled-wave equations for cSHG/DFG process. Actually, in a single PPLN waveguide, the SHG and DFG processes happen simultaneously. To simply the analysis, we assume that SHG process and DFG process is separated. In such a separated cSHG/DFG process, the pump wave is converted to SH wave firstly, and then the generated SH wave is converted to signal wave and idler wave. The coupled-wave equations for the separated cSHG/DFG process can be expressed as [2]
For SHG:

$$\begin{aligned}
\frac{dA_p}{dz} &= \frac{2i\omega_p^2 d_{\mathrm{eff}}}{k_p c^2} A_{\mathrm{SH}} A_p^* \exp(-i\Delta k_{\mathrm{SHG}} z) - \frac{\alpha_p}{2} A_p, \\
\frac{dA_{\mathrm{SH}}}{dz} &= \frac{i\omega_{\mathrm{SH}}^2 d_{\mathrm{eff}}}{k_{\mathrm{SH}} c^2} A_p^2 \exp(i\Delta k_{\mathrm{SHG}} z) - \frac{\alpha_{\mathrm{SH}}}{2} A_{\mathrm{SH}},
\end{aligned} \tag{S5}$$

And for DFG:

$$\begin{aligned}
\frac{dA_{\mathrm{SH}}}{dz} &= \frac{i\omega_{\mathrm{SH}}^2 d_{\mathrm{eff}}}{k_{\mathrm{SH}} c^2} A_s A_i \exp(-i\Delta k_{\mathrm{DFG}} z) - \frac{\alpha_{\mathrm{SH}}}{2} A_{\mathrm{SH}}, \\
\frac{dA_s}{dz} &= \frac{2i\omega_s^2 d_{\mathrm{eff}}}{k_s c^2} A_{\mathrm{SH}} A_i^* \exp(i\Delta k_{\mathrm{DFG}} z) - \frac{\alpha_s}{2} A_s, \\
\frac{dA_i}{dz} &= \frac{2i\omega_i^2 d_{\mathrm{eff}}}{k_i c^2} A_{\mathrm{SH}} A_s^* \exp(i\Delta k_{\mathrm{DFG}} z) - \frac{\alpha_i}{2} A_i.
\end{aligned} \tag{S6}$$

where the phase mismatch is defined as $\Delta k_{\mathrm{SHG}} = k_{\mathrm{SH}} - 2k_p - 2\pi/\Lambda_{\mathrm{SHG}}$ for SHG and $\Delta k_{\mathrm{DFG}} = k_{\mathrm{SH}} - k_s - k_i - 2\pi/\Lambda_{\mathrm{DFG}}$ for DFG. We solve these equations for the case of perfect phase matching, that is, $\Delta k_{\mathrm{SHG}} = \Delta k_{\mathrm{DFG}} = 0$. And α_j (j = SH, p, s, i), A_j (j = SH, p, s, i), z are the power loss coefficients, slowly varying field amplitudes and propagation distance, respectively. To get some insight into the conversion process, we simply the coupled-wave equations by assuming that the waveguide propagation losses can be ignored. d_{eff} ($= (2/\pi)\, d_{33} \approx 15.9$ pm/V) is the effective nonlinear coefficient for cSHG/DFG process. In the pump-depletion theory, the pair of coupled equations for SHG must be solved simultaneously, where the pump power is depleted and the SH power is increasing. Followed by the Manley-Rowe relations, we write the slowly varying field amplitudes for SHG process as

$$\begin{aligned} A_p(z) &= A_p(0)\,\mathrm{sech}(\zeta z), \\ A_{\mathrm{SH}}(z) &= A_p(0)\tanh(\zeta z), \\ \zeta &= \frac{2\omega_p d_{\mathrm{eff}}}{c\sqrt{n_{\mathrm{eff}}(\lambda_p)\, n_{\mathrm{eff}}(\lambda_{\mathrm{SH}})}}\left|A_p(0)\right|. \end{aligned} \tag{S7}$$

where $A_p(0)$ is the input field amplitude of pump wave, and ζ is defined as the real coupling constant for SHG process. The calculated average powers can be expressed as $P = IA_{\mathrm{eff}} = 2n_{\mathrm{eff}}\varepsilon_0 c A^2 A_{\mathrm{eff}}$, where I, A_{eff}, ε_0 are the intensity, mode effective area and vacuum permittivity, respectively. By Equation (S7) and the expression of P, we can obtain the average powers of pump and SH waves:

$$\begin{aligned} P_p(z) &= P_p(0)\,\mathrm{sech}^2(\zeta z), \\ P_{\mathrm{SH}}(z) &= \frac{n_{\mathrm{eff}}(\lambda_{\mathrm{SH}})A_{\mathrm{eff}}(\lambda_{\mathrm{SH}})}{n_{\mathrm{eff}}(\lambda_p)A_{\mathrm{eff}}(\lambda_p)}\, P_p(0)\tanh^2(\zeta z), \\ \zeta &= \omega_p d_{\mathrm{eff}}\sqrt{\frac{2P_p(0)}{\varepsilon_0 c^3 n_{\mathrm{eff}}^2(\lambda_p)\, n_{\mathrm{eff}}(\lambda_{\mathrm{SH}})A_{\mathrm{eff}}(\lambda_p)}}. \end{aligned} \tag{S8}$$

where $P_p(0)$ is the input average power of pump wave. The absolute conversion efficiency is defined as $\beta = P_{\mathrm{SH}}(z)/P_p(0)$, which is mainly determined by ζ and z. Compared to conventional PPLN, the thin-film PPLN waveguides have a much smaller mode effective area A_{eff}, which can dramatically increases the absolute conversion efficiency, as shown in Equation (S8).

Then, for DFG process, to simplify the solving of Equation (S6), we assume that the SH wave is undepleted by the nonlinear interaction, so that we can treat A_{SH} as a constant. And the boundary conditions are set as $A_s(0)$ is arbitrary, $A_i(0)$ is 0, where $A_s(0)$, $A_i(0)$ are the input slowly varying field amplitudes of signal and idler, respectively. After complex calculations, the average powers of signal and idler waves are expressed as

$$\begin{aligned} P_s(z) &= P_s(0)\cosh^2\kappa z, \\ P_i(z) &= \frac{A_{\mathrm{eff}}(\lambda_i)\omega_i}{A_{\mathrm{eff}}(\lambda_s)\omega_s}\, P_s(0)\sinh^2\kappa z, \\ \kappa &= \sqrt{\frac{2d_{\mathrm{eff}}^2\omega_s\omega_i P_{\mathrm{SH}}}{\varepsilon_0 c^3 n_{\mathrm{eff}}(\lambda_{\mathrm{SH}})\, n_{\mathrm{eff}}(\lambda_s)\, n_{\mathrm{eff}}(\lambda_i)A_{\mathrm{eff}}(\lambda_{\mathrm{SH}})}}. \end{aligned} \tag{S9}$$

where $P_s(0)$ is the input average power of signal wave, and κ is defined as the real coupling constant for DFG process. The AOWC conversion efficiency is defined as $\eta = P_i(z)/P_s(0)$, which is mainly determined by the κ and z. Compared to conventional PPLN, the thin-film PPLN waveguides can achieve much higher η at the same propagation distance z because of

the smaller A_{eff}, as shown in Equation (S9). To analyze the relationship between η and z, $P_p(0)$, we substitute the P_{SH} into Equation (S9) and obtain the η:

$$\eta = \frac{P_i(z)}{P_s(0)} = \frac{A_{\text{eff}}(\lambda_i)\omega_i}{A_{\text{eff}}(\lambda_s)\omega_s}\sinh^2 \kappa z \approx \Gamma P_p^2(0) z^4. \tag{S10}$$

where Γ represents the efficiency factor including d_{eff}, A_{eff}, n_{eff}, ω_j and some constants. We can treat the efficiency factor Γ as a constant when the waveguide dimensions and frequencies are certain. From Equation (S10) it can be seen that the AOWC conversion efficiency η depends on the second power of $P_p(0)$ and the fourth power of z. In practice, due to the waveguide propagation loss and the inhomogeneity of QPM periods, the measured η will be lower than the theoretical η. We approximately estimate that with the waveguide length L (that is, the propagation distance z) increasing from 5mm to 10mm, the η will be improved by sixteen times (about 12dB). However, all the analyses are based on the SH-undepletion theory, which is not suitable for the case of long propagation distance. When the average powers of signal and idler waves are increased to the level which is not negligible compared to the SH power, the SH-undepletion theory is no longer suitable.

The theoretical 3-dB bandwidth of AOWC conversion efficiency. In QPM PPLN waveguides, we assume that $\Delta k_{\text{SHG}} = 0$ for the case of perfect phase matching and then obtain the Λ_{SHG} by Equation (S3). When SHG and DFG processes happen simultaneously in a single PPLN waveguide, Λ_{SHG} is equal to Λ_{DFG}. As a result, the phase mismatch for DFG process can be expressed as $\Delta k_{\text{DFG}} = 2k_p - k_s - k_i$. However, when the signal wavelength is far away from the QPM wavelength, $\Delta k_{\text{DFG}} = 2k_p - k_s - k_i \neq 0$ in actual cases. Considering the $\Delta k_{\text{DFG}} \neq 0$ for DFG process, the AOWC conversion efficiency η ($\Delta k_{\text{DFG}} \neq 0$) can be written as [3]

$$\eta(\Delta k_{\text{DFG}} \neq 0) = \eta \sin c^2\left(\frac{\Delta k_{\text{DFG}} L}{2}\right). \tag{S11}$$

And the normalized η is defined as

$$\eta_{\text{norm}} = \sin c^2\left(\frac{\Delta k_{\text{DFG}} L}{2}\right). \tag{S12}$$

Figure S3 shows the normalized AOWC conversion efficiencies in 5-mm-long and 50-mm-long PPLN waveguides, respectively. The 3-dB bandwidth of η_{norm} in 5-mm-long/50-mm-long

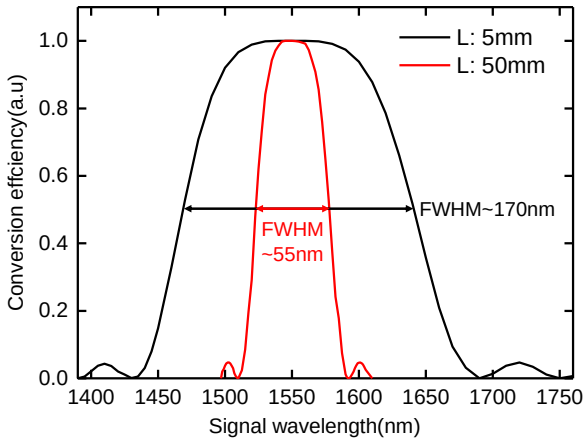

Fig. S3 The AOWC conversion efficiencies in 5-mm-long (black) and 50-mm-long (red) PPLN waveguides. FWHM, full width half maximum.

PPLN waveguide is ~170nm/55nm, respectively. Conventional PPLN waveguides require much long lengths (usually > 5cm) to achieve high AOWC conversion efficiencies due to large mode effective areas. Compared to conventional PPLN waveguides, our 5-mm-long thin-film waveguides can achieve a larger 3-dB bandwidth of η_{norm}.

References

1. Y. M. Sua, J.-Y. Chen, and Y.-P. Huang, "Ultra-wideband and high-gain parametric amplification in telecom wavelengths with an optimally mode-matched PPLN waveguide," Opt. Lett. **43**(12), 2965-2968 (2018).
2. R. W. Boyd, *Nonlinear Optics* (Academic, 2008).
3. R. Nouroozi, "All optical wavelength conversion and parametric amplification in Ti:PPLN channel waveguides for telecommunication applications," (University of Paderborn, Germany, 2010).